Comparative Numerical and Experimental Study of Taylor Bubble Dynamics in Counter-Current Flow

J. Kren*,[1], Ž. Perne*, P. Tiselj*,[1], D. Razpet*,[2]

*Reactor Engineering Division, Jožef Stefan Institute, Jamova cesta 39, 1000 Ljubljana, Slovenia
[1]Faculty of Mathematics and Physics, University of Ljubljana, Jadranska ulica 19, 1000 Ljubljana, Slovenia
[2]Faculty of Mechanical Engineering, University of Ljubljana, Aškerčeva cesta 6, 1000 Ljubljana, Slovenia

Abstract

This study investigates the behavior of Taylor bubbles in counter-current air-water flows using a dual approach of high-fidelity numerical simulations and advanced experimental techniques. The focus is on the slug flow regime, where Taylor bubbles—elongated, bullet-shaped gas pockets—occur, particularly in a scenario with a transitional Reynolds number of 1400. These bubbles present significant challenges in nuclear systems, including steam generators, during normal operations and accident scenarios such as Loss of Coolant Accidents (LOCA). Experimentally, the study analyzes three key phenomena: bubble disintegration, interface dynamics, and velocity field measurements using Particle Image Velocimetry (PIV). Numerically, a newly developed solver based on the OpenFOAM framework was employed, utilizing high-order Runge-Kutta time integration and the Volume-Of-Fluid (VOF) method to capture bubble interface dynamics with high precision. A detailed comparison between algebraic and geometric interface capturing techniques was performed. The results demonstrate good qualitative agreement between experimental and numerical velocity fields in the wake region of the bubble, with only minor quantitative discrepancies. These findings enhance the understanding of two-phase flow behavior and have important implications for improving thermal system designs in future nuclear power plants.

1. INTRODUCTION

Understanding two-phase flow dynamics is a cornerstone for the successful operation of nuclear power plants (NPPs), both under normal operating conditions and during accident scenarios. The complex behavior of two-phase flows, characterized by a wide range of flow regimes and transitions between them, remains one of the most unpredictable aspects of NPP performance. These uncertainties pose significant challenges in accurately modeling reactor behavior, particularly under transient or accident conditions, where fluid dynamics can drastically impact safety margins. Historically, early models of two-phase flows in nuclear systems relied on lumped parameter approaches, reflecting the computational limitations of the time when many of today's reactors were designed and constructed. As efforts to reduce uncertainties advanced, one-dimensional (1D) two-fluid models were introduced, forming the foundation of system codes used in nuclear safety assessments. In recent decades, however, significant progress has been made in moving toward more detailed three-dimensional (3D) modeling, which captures the intricate dynamics of two-phase flows with much greater accuracy.

This paper investigates the complex behavior of the vertical slug flow regime, a critical flow pattern that occurs in various nuclear systems, including pressurized water reactor (PWR) steam generators. Specifically, we examine the dynamics of gas slugs trapped in counter-current flow within pipes of different diameters, representative of U-tube configurations typically found in PWRs. Our case focuses on the transitional laminar-turbulent regime, where the interplay between turbulence, interface dynamics, and phenomena like bubble coalescence and breakup becomes highly influential. This investigation is an essential step toward advancing our understanding of two-phase flow heat transfer mechanisms. By employing advanced numerical simulations and experimental techniques, this work aims to reduce the uncertainties in multiphase flow predictions. Such insights are crucial not only for enhancing the safety and efficiency of current nuclear reactors but also for informing the design of next-generation thermal systems, including small modular reactors (SMRs) and other advanced nuclear technologies.

2. METHODOLOGY

2.1 Numerics

The two-phase gas-liquid mixture is modeled using a one-fluid formulation of the Navier-Stokes equations combined with the Volume Of Fluid (VOF) method for interface capturing. In this approach, a void fraction α is introduced, governed by an advection equation:

$$\frac{\partial \alpha}{\partial t} + \frac{\partial}{\partial x_i}(\alpha U_i) = 0,$$

where U_i represents the local fluid velocity, with partial time derivative ∂_t and spatial derivative ∂x_i. Across the interface, the material properties of the fluid change abruptly; however, cells in the fixed computational mesh often contain both phases, reflecting the properties of both liquid and gas. To represent these mixture properties, they are typically modeled as:

$$\rho = \alpha\rho_l + (1-\alpha)\rho_g, \quad \mu = \alpha\mu_l + (1-\alpha)\mu_g,$$

where ρ_l, μ_l and ρ_g, μ_g are the density and viscosity of the liquid and gas, respectively. This is called arithmetic mean relation for density and viscosity of the mixture.

The incompressibility constraint and the single field momentum equation read:

$$\frac{\partial U_i}{\partial x_i} = 0, \qquad and \qquad \rho\left(\frac{\partial U_i}{\partial t} + U_j\frac{\partial U_i}{\partial x_j}\right) = -\frac{\partial P}{\partial x_i} + \frac{\partial}{\partial x_j}\left[\mu_{eff}\left(\frac{\partial U_i}{\partial x_j} + \frac{\partial U_j}{\partial x_i}\right)\right] + f_{\sigma,i},$$

where P denotes the pressure field. $f_{\sigma,i} = \sigma\kappa n\delta$ denotes the surface tension force, which is solved as a continuum surface force (CSF). In this equation, σ denotes surface tension coefficient, κ curvature, n interface normal vector and δ delta function.

In this study, we focus on the finite volume method, a fundamental technique employed within the OpenFOAM framework [1]. A key contribution of this work is the development of a modified interFoam solver, which integrates Diagonally Implicit Runge-Kutta (DIRK) time integration schemes with Piecewise Linear Interface Calculation (PLIC) for geometric reconstruction. This state-of-the-art approach significantly improves the accuracy of interface tracking in two-phase flows. The primary advancement over previous work is the implementation of geometric Volume-Of-Fluid (VOF) methods, which enable sharp reconstruction of the gas-liquid interface—a level of precision not achievable with the traditional algebraic VOF method. While algebraic VOF calculates numerical fluxes to update the volume fraction α, utilizing a donor-acceptor formulation with flux limiters to maintain the boundedness of α, the geometric VOF method operates differently. It separates the interface reconstruction from its advection. First, the interface is approximated based on volume fraction data. Next, the reconstructed interface is advected according to the velocity field. For PLIC-based methods, this reconstruction process is completed in two steps, providing a much sharper interface definition [2]. Turbulence at the sub-grid scales was modeled using the Wall-Adapting Local Eddy-Viscosity (WALE) model [3], which calculates the effective viscosity μ_{eff} in Eq. 3, primarily within the bubble wake region where the flow transitions to turbulence. The fluid properties for this case were chosen to mimic a water-air mixture, and the pipe geometry consisted of a 12.4 mm diameter and a 24.8 cm length. A recycling boundary condition was applied at the inlet—upstream of the Taylor bubble—to ensure fully developed flow. Additionally, the flow rate was dynamically adjusted at each timestep to maintain a near-zero net force on the bubble, ensuring its buoyancy was balanced by the hydrodynamic drag, thereby keeping it in a constant position throughout the simulation. The simulations ran on our in-house cluster, utilizing approximately 200 cores over the course of one month. This numerical case was also replicated experimentally.

2.2 Experiments

At the THELMA laboratory, part of the Reactor Engineering Division at the Jožef Stefan Institute, a dedicated test section was constructed, as shown in Figure 1. In this setup, several parameters, including absolute pressure, pressure drop across the section, temperature, and water flow rate, were monitored. High-speed visual measurements were conducted using a high-speed camera and laser equipment. Further details about the experimental setup can be found in the Master's thesis of Žiga Perne and the PhD thesis of Jan Kren.

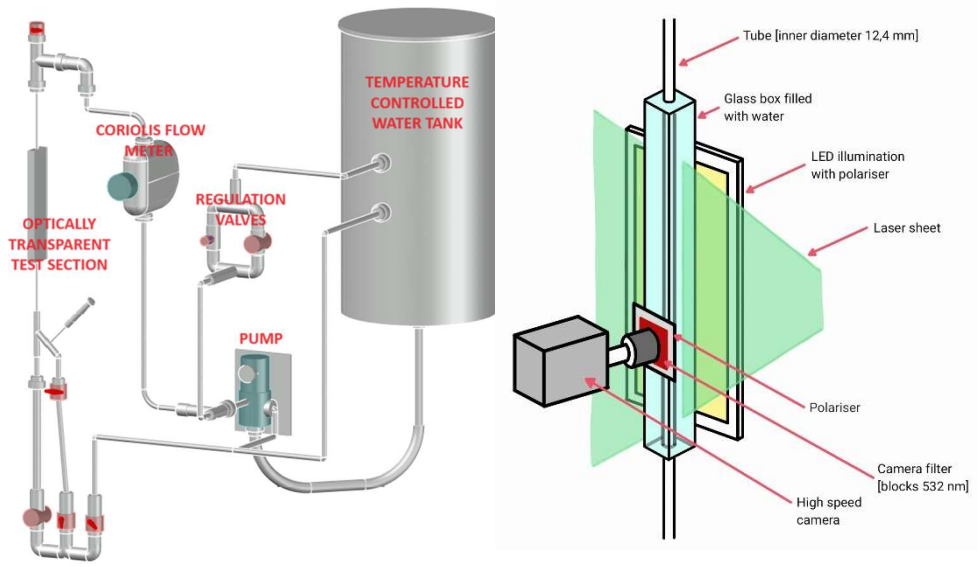

Figure 1: Three-dimensional scheme of the experimental device (left) and of the PIV setup (right).

A quick overview of the experimental efforts can be seen in the Figure 2. We have created and implemented a dynamic masking algorithm, which utilized our knowledge of interface detection in LED light illuminated images, first developed for study of bubble shapes and interface waves [4]. This approach leverages the short interval between laser shots to create a dynamic masking effect, enhancing the accuracy of interface detection. The mask is necessary to mitigate reflections occurring at the Taylor bubble interface and along the pipe walls, which might interfere with the accuracy of the PIV algorithm. The modified algorithm better adapts to the challenges of capturing the Taylor bubble's interface in varying lighting conditions as to the previous unsuccessful attempt to create masks directly from PIV images [5].

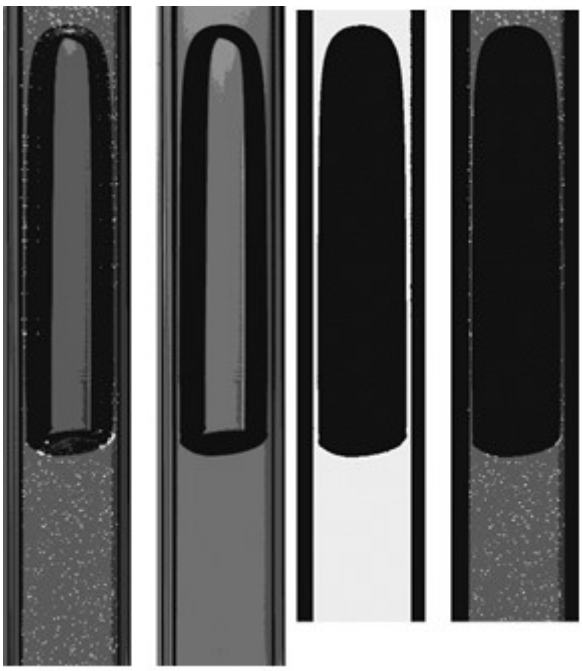

Figure 2: Dynamic Masking in PIV of Taylor bubble in counter-current flow: Left to right: ***1:*** *raw image with laser illumination,* ***2:*** *raw image with ambient LED illumination,* ***3:*** *mask created from the LED illuminated image,* ***4:*** *mask merged with the PIV image, prepared for PIV processing.*

3. RESULTS

The combined numerical and experimental efforts enabled a direct comparison of measurements and simulations. Figure 3 presents the isosurfaces of instantaneous gas volume fraction at α = 0.5 for two distinct interface capturing methods, shown at one timestep at t = 10 s. On the right, an experimental photograph shows a Taylor bubble of similar length for reference. A notable difference between the two methods is the behavior of the gas volume shedding. The algebraic VOF method predicts significant gas shedding and bubble breakup, whereas the geometric VOF method maintains a stable bubble without any breakup, which is in good agreement with the experimental observations [6]. Furthermore, substantial differences between the two methods are observed in the velocity fields within the bubble's wake region, as also illustrated in Figure 3. With the geometric VOF method, the wake exhibits an organized, recirculating flow pattern trailing behind the bubble. In contrast, the algebraic VOF method predicts a highly disordered wake. Here, multiple smaller bubbles form and proliferate, disrupting the flow and contributing to a more turbulent and chaotic velocity

field. This chaotic behavior leads to increased randomness in the flow patterns, introducing greater perturbations and making the velocity field more erratic.

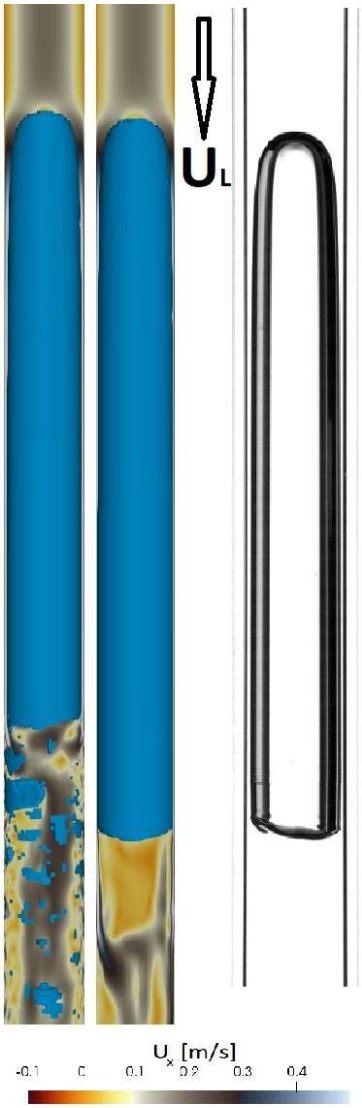

Figure 3: Isosurfaces of the instantaneous gas volume fraction (blue color) at t = 10 s time, obtained with standard algebraic interface capturing (left) and PLIC reconstruction (middle) for transitional case (Re = 1400). The color scheme in the liquid phase represents the velocity magnitude. On the right side photo of Taylor bubble in counter-current flow from experiment [7].

Figure 4 presents a comparison of two-dimensional contour plots of the Taylor bubble wake, showing both the streamwise (lower plots) and radial (upper plots) velocity fields derived from simulations (left plots) and experimental data (right plots). Both plots use the same color scale to ensure consistency across the graphs. The numerical data is based on our finest mesh, containing approximately 5 million cells, while the experimental data corresponds to the largest observed bubble, with a length of 4.3 D_h.

In contrast, the bubble in the numerical simulations was significantly larger, measuring 8.1 D_h. Despite this difference in bubble size, the comparison focuses on the velocity fields in the bubble wake region, where the flow structures and velocity patterns remain comparable. In both datasets, a turbulent jet emerges at similar positions, indicating good agreement in the general flow structure. Additionally, both the simulated and experimental data display axial symmetry, further supporting the consistency between the two approaches. However, several differences are notable. The experimental data appears coarser, with fewer refined details compared to the simulations, which reveal more intricate flow features. Some structures visible in the numerical results are less pronounced or harder to discern in the experimental data. Moreover, the extreme values in the radial velocity field in the experimental data are shifted slightly downstream compared to the numerical results, suggesting potential discrepancies in the precise positioning of flow features. Overall, while the experimental data confirms the general trends seen in the simulations, it lacks some of the finer details captured in the numerical results. This highlights the ability of numerical simulations to resolve complex flow phenomena with greater precision while also emphasizing the critical role of experimental validation in ensuring the accuracy of high-resolution flow characterization.

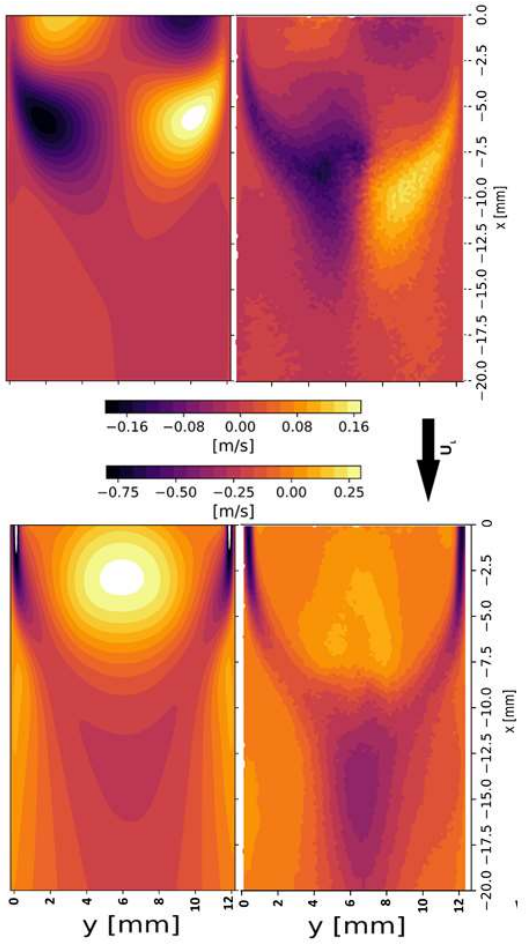

Figure 4: Streamwise (bottom) and radial (top) velocity in the Taylor bubble wake for the simulations (left) and experiment (right).

For a detailed quantitative comparison, we examined the velocity profiles at three different cross-sections (-2 mm, -5 mm and -15 mm from the Taylor bubble rear end) in the Taylor bubble wake region as shown at the bottom of Figure 5 for the finest numerical mesh and for the longest experimental Taylor bubble. Due to the ambiguity in precisely defining the Taylor bubble's rear end position in the

experiments, uncertainties have been included in the figures. These uncertainties, set at ± 2 mm, account for the fluctuating position of the bubble's trailing edge over time. To improve visualization and interpretation, an envelope was created around the main profile. Figure 5 displays the streamwise velocity component (left) and radial velocity component (right) at the specified positions. Overall, the two methods show strong alignment, though some deviations appear further from the Taylor bubble's rear end and at greater distances from the wall. These discrepancies are primarily attributed to the steep velocity gradients in this region, which introduce additional uncertainties. Despite these variations, the critical flow characteristics, such as the liquid jet emerging from the liquid film region (seen in the profile at x = - 2 mm) and secondary vortex observed as positive velocity at x = - 15 mm, are clearly visible and well-defined. On the right side of Figure 5, the radial velocity profiles at the same positions are presented. Near the Taylor bubble, the velocity fields show strong agreement, but as the distance from the bubble increases, the velocities begin to diverge slightly.

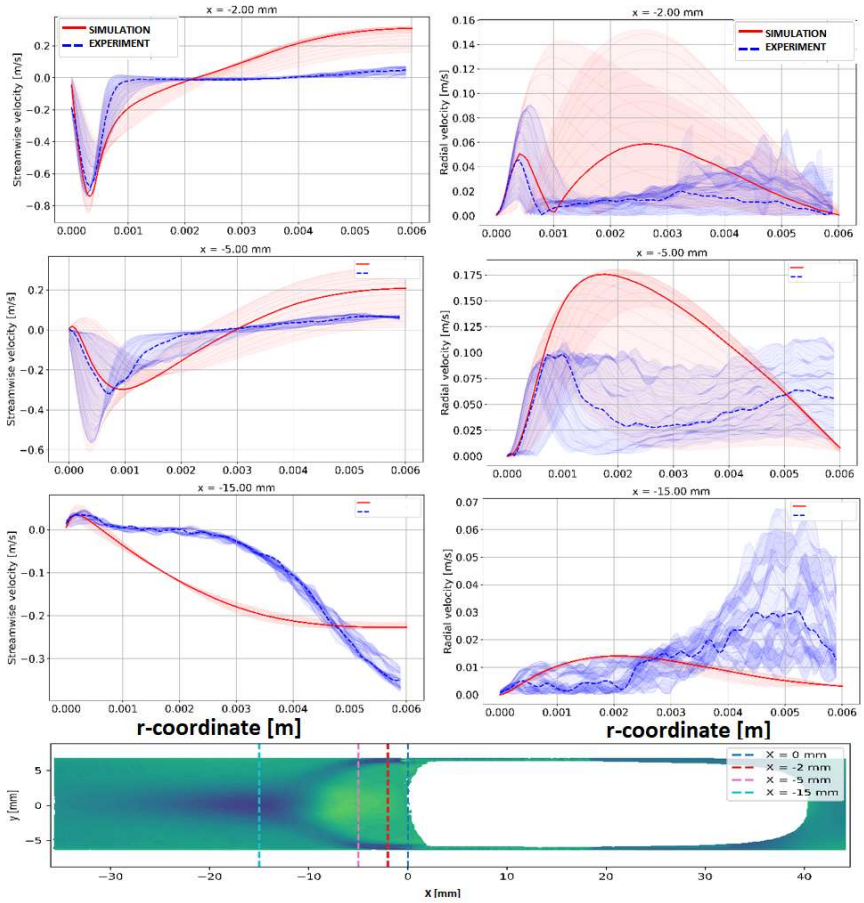

Figure 5 Left: Streamwise velocity at two different positions for experimental (blue) and numerical (red) case. Right: Radial velocity at three different positions. Bottom: Locations of the profiles shown in the above graphs.

The uncertainty of the cross-section position with respect to the Taylor bubble is considerable, making it essential to include an envelope around the bubble in our analysis to account for this variability. Several factors contribute to the discrepancies observed in Figures 4 and 5, each impacting the flow dynamics in distinct ways. One of the primary sources of discrepancy lies in the difference in bubble size between the experimental and simulated cases. The experimental bubble measures approximately 4.3 D_h, while the simulated bubble is significantly larger at 8.1 D_h. This variation in bubble size is likely to influence flow dynamics, particularly regarding the intensity of turbulence and the wake effects that develop around the bubble. Both turbulence and wake characteristics are highly sensitive to the size and shape of the bubble, making size discrepancies a key factor in explaining differences in the observed results. Another contributing factor is the variation in boundary conditions and flow configurations between the experimental and numerical setups. Small differences in parameters such as inlet flow rate and pressure conditions can lead to distinct flow characteristics. Even slight discrepancies in flow rate, on the order of a few percentage points, may alter the turbulence downstream of the bubble, leading to deviations in the velocity profiles and overall flow behavior. Variations in inlet boundary conditions further complicate the comparison, as they can introduce subtle but impactful differences in the flow regime. Lastly, limitations inherent to the experimental setup could also explain some of the discrepancies observed. Experimental setups often face constraints such as shorter time-averaging windows, potential light distortions when observing through the test section, and resolution limitations in capturing fine flow details. These factors can reduce the accuracy and precision of experimental data, particularly in regions farther from the bubble where interactions are more complex and sensitive to setup nuances. Collectively, these factors help explain the observed discrepancies in the velocity

profiles, especially in regions distant from the bubble. In these areas, flow interactions become increasingly sensitive to the specific characteristics of each setup, whether experimental or numerical, highlighting the challenges inherent in comparing these two approaches directly.

4. CONCLUSIONS

This study advances critical insights into Taylor bubble dynamics within vertical counter-current air-water flows, emphasizing the comparison between high-resolution experimental observations and high-fidelity numerical simulations, particularly in the velocity fields in the bubble's wake. This work directly supports improved modeling accuracy for multiphase flows in nuclear safety applications, where the behavior of gas-liquid interfaces under counter-current flow conditions is essential to reactor safety assessments. Building on previous research by Kren et al. (2023, 2024) [4], [7], significant progress was achieved through several key developments in both experimental and numerical methods. These advancements include:

- Precision in reconstructing gas-liquid interfaces in Taylor bubble images under LED illumination,
- Development of a dynamic masking algorithm to enhance Particle Image Velocimetry (PIV) data processing,
- High-fidelity numerical simulations capturing Taylor bubble behavior in counter-current flow conditions,
- Implementation of the geometric Volume-Of-Fluid (VOF) method with Runge-Kutta time-integration, embedded in the newly developed interRKFoam solver,
- Establishment of a systematic methodology for robust comparison between experimental and numerical data.

These improvements allow a detailed analysis of velocity fields in the wake of Taylor bubbles, effectively bridging experimental and computational approaches—a critical step for refining multiphase flow models used in nuclear safety assessments. The strong agreement observed between experimental and numerical results highlights the accuracy and reliability of these methods, reinforcing their application to reactor thermal-hydraulics modeling and safety validation.

The findings underscore the importance of such advanced two-phase flow models for Technical Safety Organizations (TSOs), providing a foundation for more accurate simulations that support the design, safety margins, and risk assessment of nuclear reactors. This work further contributes to nuclear safety research, supporting TSOs in advancing best practices and reliable methodologies in reactor safety and accident analysis.

Acknowledgements

The authors would like to express their gratitude to Dr. Blaž Mikuž and Prof. Dr. Iztok Tiselj for their invaluable contributions to the conceptualization, supervision, and guidance provided throughout the work presented in this paper. This work has been financially supported by the Slovenian Research Agency (ARIS) and by the Reactor Engineering Division of Jožef Stefan Institute (research core funding No. P2-0026 ``Reactor Engineering'').

References

[1] The OpenFOAM Foundation, “OpenFOAM | Free CFD Software.” Accessed: Jan. 05, 2022. [Online]. Available: https://openfoam.org/
[2] C. W. Hirt and B. D. Nichols, “Volume of fluid (VOF) method for the dynamics of free boundaries,” *J. Comput. Phys.*, vol. 39, no. 1, pp. 201–225, Jan. 1981, doi: 10.1016/0021-9991(81)90145-5.
[3] S. B. Pope, *Turbulent flows*. Cambridge ; New York: Cambridge University Press, 2000.
[4] J. Kren *et al.*, “Dynamics of Taylor bubble interface in vertical turbulent counter-current flow,” *Int. J. Multiph. Flow*, vol. 165, p. 104482, Aug. 2023, doi: 10.1016/j.ijmultiphaseflow.2023.104482.
[5] J. Kren and B. Mikuž, “Large interface tracking algorithm for air-water slug in turbulent flow,” p. 8, 2021.
[6] B. Mikuž, J. Kamnikar, J. Prošek, and I. Tiselj, “Experimental Observation of Taylor Bubble Disintegration in Turbulent Flow,” *Proc. 28th Int. Conf. Nucl. Energy New Eur.*, p. 9, 2019.
[7] J. Kren, E. M. A. Frederix, I. Tiselj, and B. Mikuž, “Numerical study of Taylor bubble breakup in counter-current flow using large eddy simulation,” *Phys. Fluids*, vol. 36, no. 2, p. 023311, Feb. 2024, doi: 10.1063/5.0186236.